PERFORMANCE ANALYSIS OF ADJUSTABLE-TILT TILTED SINGLE-AXIS VERSUS HORIZONTAL SINGLE-AXIS TRACKERS: A BRAZILIAN PV PLANT CASE STUDY

Eslam Mahmoudi[1], João Lucas de Souza Silva[1], Gustavo Fraidenraich[2], Denis G. Fantinato[3] and Tárcio André dos Santos Barros[1]

[1] Department of Energy and Systems, FEEC, Universidade Estadual de Campinas, Campinas, Brazil.

[2] Department of Communications, FEEC, Universidade Estadual de Campinas, Campinas, Brazil.

[3] Department of Computer Engineering, FEEC, Universidad Estadual de Campinas, Campinas, Brazil.

Abstract

This study evaluates whether reconfiguring horizontal single-axis trackers (HSATs) into tilted single-axis trackers (TSATs) can enhance plane-of-array (POA) irradiance capture. To this end, three TSATs—annual, seasonal, and monthly adjustable-tilt—are designed, with their tilt angles set to optimal values for corresponding period to their maximum aggregate POA values, derived from hourly POA estimates obtained using an optimal combination of decomposition and transposition models. The relative performance of adjustable-tilt TSATs is then compared with HSAT to quantify potential gains in captured POA irradiance.

Numerical simulations are conducted for a PV plant equipped with HSATs in Dracena, Brazil. Ground-truth data are used to identify the optimal combination of decomposition and transposition models from 400 combinations. This combination is applied to determine the optimal tilt angles for adjustable-tilt TSATs, calculate their POA on annual, seasonal, and monthly timescales, and compare the resulting POA values with those of the HSAT across the same periods. Simulation results show that while the annual fixed-tilt TSAT does not consistently outperform the HSAT, the monthly adjustable-tilt TSAT consistently yields higher POA values. All three TSAT configurations exceed HSAT performance during March, April, May, June, July, and September, with the monthly adjustable-tilt TSAT achieving the highest improvement of 25.61% in June.

Keywords: Horizontal single-axis tracker, tilted single-axis tracker, adjustable-tilt tilted single-axis tracker, Plane-of-array irradiance.

1. Introduction

The global demand for renewable energy has been increasing rapidly. Photovoltaic (PV) systems, as one of the leading renewable energy technologies, provide substantial benefits for electricity generation. They effectively address critical issues in energy security, environmental sustainability, and economic development (Campion et al. 2025). PV power emerged as a significant energy source in Brazil in 2012, and by the end of November 2024, total installed capacity had reached 50.67 GW, of which 16.64 GW was from centralized plants and 34.03 GW from distributed installations (ABSOLAR, 2025). PV systems with fixed-tilt arrays and horizontal single-axis trackers (HSATs) are the most widely installed in Brazil.

A PV module is the essential element of a PV system, designed to capture sunlight and convert it into electricity. The performance of a PV system is significantly influenced by the positioning of the PV modules, specified by their tilt and azimuth angles (Mahmoudi et al. 2023a). PV systems comprise PV modules that are typically installed at fixed optimal tilt and azimuth angles (Mahmoudi et al. 2023b). However, the fixed-tilt PV arrays often fail to achieve optimal POA irradiance. Implementing sun-tracking systems is a highly effective approach to maximizing POA received by PV modules. Numerous studies (Sanyal et al. 2024; Alomar et al. 2023; Gönül et al. 2022; Berrian et al. 2019; Bahrami et al. 20117) have consistently shown that HSAT and dual-axis trackers (DAT) outperform fixed-tilt PV arrays. For instance, Alomar et al. (2023) have shown that the energy produced by HSAT and DAT increases by 16.5% and 25.5%, respectively, compared to a fixed PV array. Moreover, these studies confirm that the DAT performs better than HSATs. However, due to the higher capital investment and

10.18086/swc.2025.01.19 Available at http://proceedings.ises.org

maintenance costs associated with DATs, the HSATs are often considered a more economically viable option for PV plants. To enhance performance without incurring substantial additional costs, HSATs can be reconfigured as tilted single-axis trackers (TSATs), characterized by an axis of rotation inclined between the horizontal and vertical planes. Zhimin et al. (2010) investigated the optical performance of inclined south–north single-axis tracked panels versus fixed-tilt systems using annual collectible radiation and found that the inclined tracker performed better. Ray and Tripathi (2016) designed, implemented, and experimentally tested TSATs and DATs, finding that TSATs outperformed HSATs. Bahrami et al. (2022) compared the performance of several single-axis tracker types —east-west, north-south, inclined east-west (IEW), and vertical-axis —using the IEW tracker set to its annual optimal slope. They found that the IEW tracker, when set at its annual optimal inclination, outperformed HSATs but remained inferior to DATs.

Furthermore, irradiance datasets at the desired location are essential for estimating POA irradiance for fixed-tilt and sun-trackers. Solarimetric stations in PV systems play a crucial role in identifying issues and evaluating performance by providing data for simulations (De Souza Silva et al, 2023). Despite the importance of local solarimetric station data for assessing PV plant performance and improving simulation accuracy (De Souza Silva et al, 2024; De Souza Silva et al, 2025), many locations lack such infrastructure. Consequently, satellite-based datasets are widely used to evaluate PV plant performance.

The literature review shows that few studies have investigated TSATs and compared them with HSATs. Most of these works focused on the annual optimal tilt for TSATs and do not examine monthly or seasonal optimal tilts. This study addresses this gap by presenting a simulation framework to evaluate the potential performance enhancement of HSATs through their reconfiguration into adjustable-tilt TSATs to maximize captured POA irradiance. Compared with previous works, the main contributions of this paper are summarized as follows:

(1) Unlike prior studies that employed random or recommended combinations of physical decomposition and transposition models, this work performs Global Horizontal Irradiance (GHI) to POA conversions for single-axis trackers using 400 combinations derived from 20 decomposition and 20 transposition models. These combinations are evaluated against measured GHI and POA data from the Dracena PV plant equipped with HSAT. The best-performing model combination is identified through statistical analysis for use in subsequent simulations.

(2) Departing from previous studies that used a single optimal tilt for TSATs, this study introduces adjustable-tilt TSATs, where the tilt angle is optimized monthly to maximize the corresponding POA. The identified best-performing model combination is used to estimate hourly POA values, which are then aggregated at monthly, seasonal, and annual timescales to determine the optimal tilt angles for TSATs for each period. Accordingly, the proposed simulation framework quantifies the POA irradiance gains achieved by reconfiguring HSAT into adjustable-tilt tilted TSATs set at their optimal tilt angles.

2. Methodology and Materials

2.1. Solar geometry

The intensity of solar radiation is closely linked to the sun's position relative to an observer on Earth's surface. The geometric relationships between a plane of any given orientation and Earth can be described using a series of angles, whether the plane is stationary or in motion relative to Earth. Figure. 1 provides a visual representation of these angles.

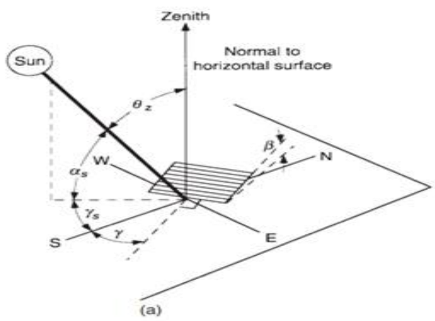

Figure 1. Solar position angles.

The following parameters define the solar positions.

- Longitude (L): The angular position to the west of Greenwich is represented within the range of $0^{\circ}$to 360°. If longitude is specified using the convention of (-180°≤ $L \leq$ +180°), it can be converted to the textual convention by taking the absolute value of a negative longitude or subtracting the provided positive longitude from 360°.
- Latitude (φ): The angular position with respect to the equator is denoted as north or south, where north is positive. The range of values is -90°≤ $\varphi \leq 90^{\circ}$.
- Declination (δ): The Sun's angular position at solar noon (when the sun is on the local meridian) relative to the equatorial plane, with north as the positive direction. The range of values for declination is -23.45° $\leq \delta \leq 23.45^{\circ}$. Solar declination arises from the slight tilt of the Earth's axis, which is approximately 23.45º with respect to its elliptical axis.
- Tilt (β): the angle between the inclined surface plane and the horizontal plane, 0°≤ $\beta \leq 90^{\circ}$. The tilt angle $90^{\circ} < \beta$ indicates that the surface possesses a downward-facing aspect.
- Surface azimuth angle (γ): The difference between the projection of the surface's normal onto a horizontal plane and the local meridian, with zero representing due south, east as negative, and west as positive. The range for this deviation is -180°≤ $\gamma \leq$ +180°.
- Hour angle (ω): The angular displacement of the sun to the east or west of the local meridian results from the Earth's rotation on its axis, occurring at a rate of 15 degrees per hour. A negative value indicates the morning, while a positive value indicates the afternoon.
- Incidence angle (θ_i): The angle between the beam radiation on a surface and the normal to that surface.
- Zenith angle (θ_z): The angle between the vertical direction and the line connecting to the sun, also known as the angle of incidence for beam radiation on a horizontal surface.
- Solar elevation angle (α_s): The angle between the horizontal plane and the line connecting to the sun essentially complements the zenith angle. The α_s is the complement of θ_z.
- Solar azimuth angle (γ_s): The angular displacement from the southward direction of the projection of beam radiation on the horizontal plane. Negative values represent displacements to the east of the south, while positive values indicate displacements to the west of the south.

This study employs the PVlib Python package (Anderson et al. 2023) to calculate the solar positions at hourly and sub-hourly intervals.

2.2. Horizontal single-axis tracker

A solar tracker is a device that orients the PV modules toward the sun to increase PV system efficiency and conversion rate. The trackers are used to minimize the angle of incidence between the incident sunlight and the surface of the PV panel, i.e., θ_i, resulting in optimizing the energy yield. An HSAT rotates from east to west about a fixed axis parallel to the ground and aligned with a north-south line. The PV modules are mounted on the HSAT and rotate about their axes to track the apparent motion of the Sun throughout the day.

2.3. Tilted and adjustable-tilt tilted single-axis trackers

Solar trackers with an axis of rotation inclined between the horizontal and vertical planes are referred to as TSATs. The PV module surface is oriented parallel to the rotation axis, and as the tracker follows the apparent motion of the Sun, the modules move along a cylindrical trajectory that is symmetric about the rotational axis. The tilt angle of a TSAT should be optimized rather than fixed at the site latitude to maximize energy yield compared with conventional HSATs. To address this, the present study introduces an adjustable-tilt TSAT configuration, in which the tilt angle dynamically varies on a monthly or seasonal basis to enhance system performance and solar energy capture further.

2.4. POA estimating for single-axis trackers

In the absence of measured POA data for HSAT and TSAT systems, the POA values can be estimated using a combination of decomposition and transposition models. Decomposition models are employed to separate the GHI into its Direct Normal Irradiance (DNI) and Diffuse Horizontal Irradiance (DHI) components. These components are subsequently transposed onto the tilted surfaces of PV modules to estimate the corresponding POA irradiance. Decomposition models have been developed for both hourly and minutely irradiance data. Most models prior to 2015 were calibrated using hourly data, whereas more recent approaches increasingly target minute-level resolution. In contrast, transposition models have been developed solely from hourly datasets. Applying hourly-calibrated models to minute-level data—or combining minutely resolved decomposition models with hourly transposition models—can introduce significant errors in POA irradiance estimates and, by extension, PV performance simulations. To avoid these pitfalls, this study restricts its analysis to decomposition and transposition models that are both calibrated and modeled at the hourly timescale.

The extensive validation conducted by Gueymard and Ruiz-Arias (2016) provides strong support for selecting 30 of the most validated decomposition models for this study. Moreover, thirty transposition models, encompassing nearly all currently available models validated by Mahmoudi et al. (2024), are selected for combination with the chosen decomposition models. Table 1 presents these models; due to space limitations, the corresponding mathematical equations are not included here, but detailed descriptions of the equations for each model can be found in the original references listed in the table.

Table 1: Decomposition and transposition models

Decomposition models	Transposition models
Orgill-hollands-1982	Liu-1963
Erbs-1982	Klucher-1979
Disc-1987	Steven1-1979
Skartveit-1987	Steven2-1979
Hollands-1987	Steven3-1980
Skartveit3-1998	Steven4-1980
DeMiguel-2001	Hay&Davies-1980
Dirindex-2002	Koronakis-1986
Mondol1-2005	Skartveit-1986
Mondol2-2008	Perez1-1987
Boland2-2008	Perez2-1988
BRL-2010	Perez3-1990
Ruiz&Arias-2010	Perez4-1990
Muneer-1990	Reindl-1990
Yao2-2013	Muneer-1990
Boland5-2013	Olmo-1999
Engerer2-2015	Muneer-2004
Abreu-2016	Evseev&Kudish, 2009
Paulescu-2016	DOE2-2010
Every1-2020	King-2012

GHI-to-POA conversion is achieved by sequentially applying decomposition and transposition models. First, GHI (G_h) data is separated into its DHI (D_h) and DNI (B_n) by:

$$D_h = f_d \times G_h \qquad \text{(eq. 1)}$$

$$B_n = \frac{G_h - D_h}{\theta_z} \qquad \text{(eq. 2)}$$

Where decomposition factor, f_d, is determined by one of the decomposition models presented in Table 1. These irradiance components are then transposed onto the inclined PV module plane, tilted by β_p and oriented at the azimuth angle γ_p, to estimate the global POA irradiance (POA_{glb}):

$$POA_{glb} = POA_b + POA_g + POA_d \qquad \text{(eq. 3)}$$

The tilted beam irradiance, POA_b, is purely geometrical and is given by:

$$POA_b = B_n \cos\theta_i \qquad \text{(eq. 4)}$$

The tilted ground-reflected irradiance, POA_g, is typically approximated as isotropic and calculated from the GHI and the ground albedo ρ :

$$POA_g = G_h \, \rho \frac{1-\cos\beta_p}{2} \qquad \text{(eq. 5)}$$

The tilted sky diffuse irradiance, POA_d, is calculated based on D_h irradiance with

$$POA_d = D_h \, . R_d \qquad \text{(eq. 6)}$$

Where, R_d denotes the diffuse transposition factor, calculated using one of the transposition models presented in Table 1.

The GHI-to-POA conversion framework is further extended to accommodate sun-tracking systems. HSAT operates by rotating the PV array on a north-south aligned horizontal axis. This rotational movement enables the system to track the sun's apparent east-west diurnal path, primarily minimizing the incidence angle to optimize POA irradiance. This study employs the HSAT model established by Anderson et al (2022) to determine the dynamic tilt β_{pt} and azimuth γ_{pt} angles of the PV modules mounted on the HSAT plane. The model incorporates solar zenith and azimuth angles to calculate the optimal tracker rotation angle θ_t through minimization of the incidence angle θ_i, from which the corresponding tilt and azimuth angles of the tracker-mounted PV modules are derived.

2.5. Optimal tilt angles for adjustable-tilt TSAT

The optimal tilt angle for adjustable-tilt TSATs , T_{opt}, over a given time period is defined as the angle that maximizes the ratio of the aggregated POA irradiance, $POA_{glb,agg}$, to the corresponding aggregated GHI, $G_{h,agg}$, during that period, by

$$T_{opt} = \max_{0\sim 90} \frac{POA_{glb,agg}}{G_{h,agg}} \qquad \text{(eq. 7)}$$

This study designs TSATs under three scenarios: annual adjustable-tilt TSAT, seasonal adjustable-tilt TSAT, and monthly adjustable-tilt TSAT. The optimal tilt angles for these TSATs in each year, month, and season are determined using Equation (7).

2.6. Comparative analysis of adjustable-tilt TSAT with HSAT

A comparative analysis is conducted to evaluate the performance of adjustable-tilt TSATs versus HSATs, using real-world data from an HSAT-equipped PV plant in Brazil. The overall simulation steps are summarized below:

- The HSAT is modeled using hourly solar position data to determine the hourly tilt and azimuth angles of the mounted PV array. These angles are then fed into an optimal decomposition and transposition models' combination for the PV location to convert GHI into hourly POA irradiance. To identify the optimal combination, a total of 400 model combinations—combining 20 decomposition and 20 transposition models— are implemented and validated against measured POA data from an HSAT-equipped PV plant in Dracena, Brazil. The best-performing combination is then identified through statistical analysis for use in subsequent simulations.
- The selected best-performing combination is then applied to estimate hourly POA values for the TSAT, where the tilt angle varies from 0° to 90° in 1° increments. These hourly POA values are aggregated to monthly, seasonal, and annual scales to determine the optimal tilt angles that maximize POA irradiance at each respective time scale.
- Three TSATs are designed, including annual adjustable-tilt, seasonal adjustable-tilt and monthly adjustable-tilt, which are adjusted at optimal tilt angles at annual, seasonal and monthly intervals, respectively.
- Each TSAT uses the best-performing combination to estimate hourly POA data, which is then aggregated into annual, seasonal, and monthly POA values.

- The performance of each TSAT is compared to the HSAT at annual, seasonal, and monthly time scales, based on their respective POA values, to calculate the percentage differences, representing either enhancement or diminishment in POA for each period, which are calculated as the improvement ($Imp\%$) by

$$Imp = \frac{POA_{TSAT} - POA_{HSAT}}{POA_{HSAT}} \times 100 \qquad \text{(eq. 8)}$$

3. Simulation results and analysis

3.1. Data

The required data for simulation and evaluation comprises radiometric and meteorological data, as well as non-radiometric information. The radiometric data are adapted from an HSAT-equipped PV plant located in Dracena, Brazil. The PV plant equipped with HSAT is in the municipality of Dracena, São Paulo, and consists of 3 units, each with 90,720 modules arranged in 3,024 strings of 30 modules, and eight inverters. The ground-measured radiometric datasets, including GHI and POA, recorded at 15-minute intervals from January 1 to December 31, 2020, are used in this study for numerical simulations. The 15-minute GHI data is averaged to hourly values for use in decomposition and transposition models. In addition, the 15-minute POA data is averaged to the hourly time step to validate against hourly-estimated POA values. The non-radiometric data for simulation consists of solar positions, as well as air mass (*A.M*) and the solar incidence angle (θ_i), which are calculated by functions in Pvlib. These are calculated for the Dracena plant location over 2020.

3.2. Evaluating the decomposition-transposition combinations

GHI and POA measurements from the Dracena PV plant are used to identify the best-performing model combinations from 400 decomposition-transposition combinations presented in Table 1 for further simulations. To this end, the hourly POA values for 400 combinations are estimated from GHI measurements and evaluated against hourly measured POA values. The evaluations are conducted using the statistical metrics, including *nMAE*, *nRMSE*, and R^2. Because no single combination can simultaneously minimize *nMAE* and *nRMSE* while maximizing R^2, Pareto-optimal combinations that trade off these objectives were identified, which are illustrated in Figure 2.

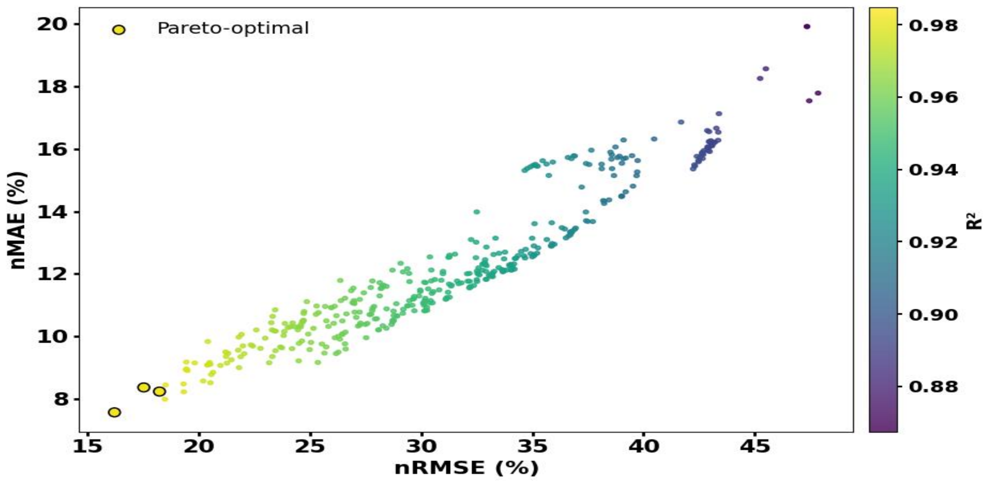

Figure 2. Scatter plots of nMAE versus nRMSE for the tracker-equipped PV plant in Dracena, SP.

Figure 2 presents scatter plots of *nMAE* versus *nRMSE* for all model combinations, with color indicating R^2 Values and black circles denote the Pareto-optimal selections. Accordingly, three Pareto-optimal model combinations were identified: Boland5 (2013) & Perez (1987), Skartveit (1987) & Perez (1988), and Boland5 (2013) & Perez (1990). The Boland5 (2013) & Perez (1987) combination was the best combination, achieving *nMAE* = 7.56, *nRMSE* = 16.2, and R^2 = 0.98.

3.1. POA estimation by best-performing combination

The best-performing combination, Boland (2013) and Perez (1987), is used to estimate hourly POA values for 2020. Figures 3 and 4 show comparisons of the aggregate monthly and seasonal simulated POA values versus measured values, respectively, derived from hourly POA values.

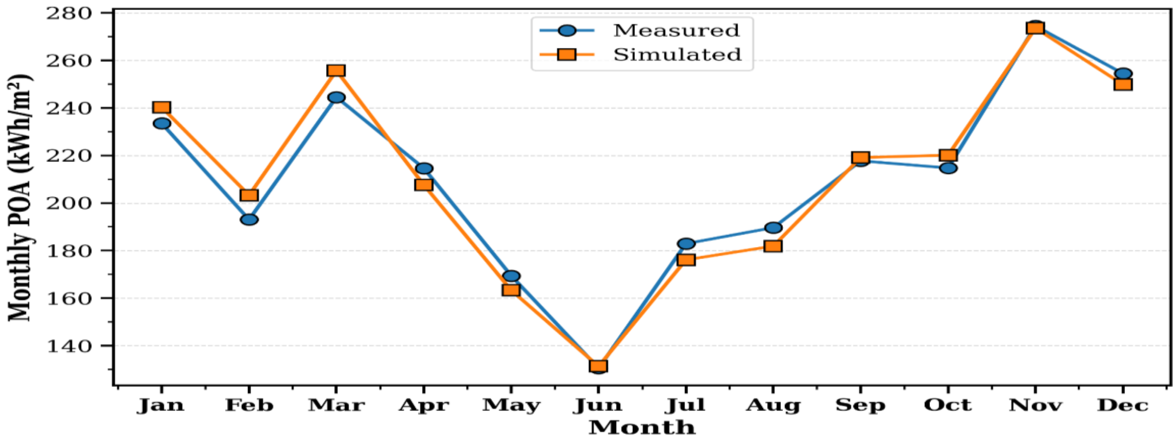

Figure 3. Monthly comparison of simulated and measured POA irradiance at Dracena PV plant.

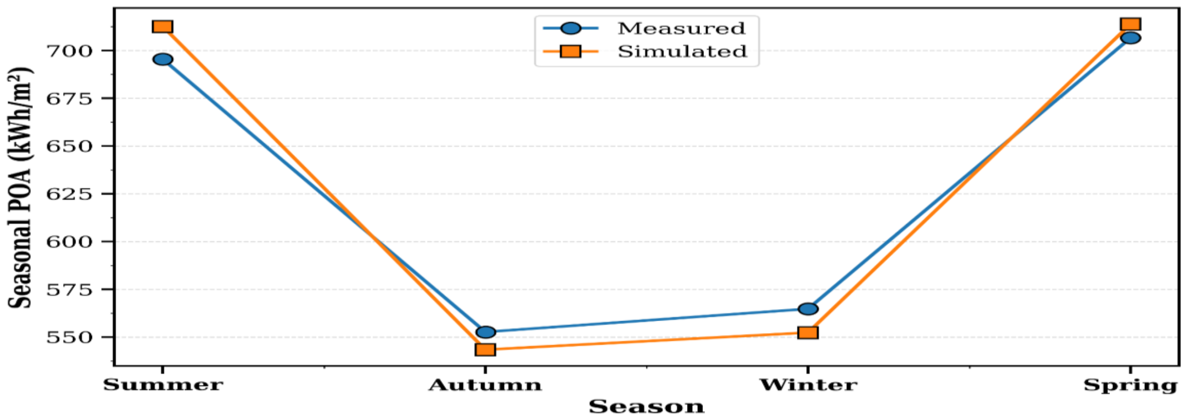

Figure 4. Seasonal comparison of simulated and measured POA irradiance at Dracena PV plant.

The hourly POA values for adjustable-tilt TSAT are estimated using GHI measurements, non-radiometric information, and a single-axis tracker model adjusted for TSAT tilt and the tracker's north-facing azimuth angle.

3.1. Optimal tilts for adjustable-tilt TSATs

The tilt angle of the TSAT is changed from $0^{\circ}$to 90° with interval 1°, and for each, the hourly POA values over 2020 are calculated, resulting in an array of 91×8784. For annual adjustable-tilt TSAT, the optimal annual tilt angle for TSAT is obtained as 23° by maximizing the annual POA from a 91×1 aggregated POA matrix over possible tilt angles $0^{\circ}$to 90° , as shown in Figure 5.

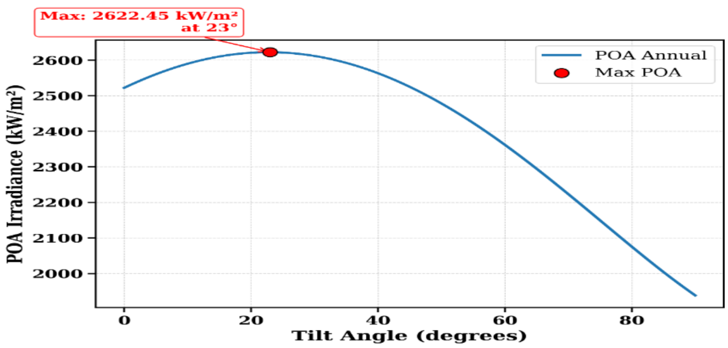

Figure 5. Optimal annual tilt angle for annual fixed-tilt TSAT

Similarly, for each season, the optimal tilt angle for adjustable-tilt TSAT is obtained by maximizing aggregated POA in the corresponding season from a 91×4 matrix, which are 4°, 40°, 41°, and 4° for Summer, Autumn, Winter, and Spring, as shown in Figure 6.

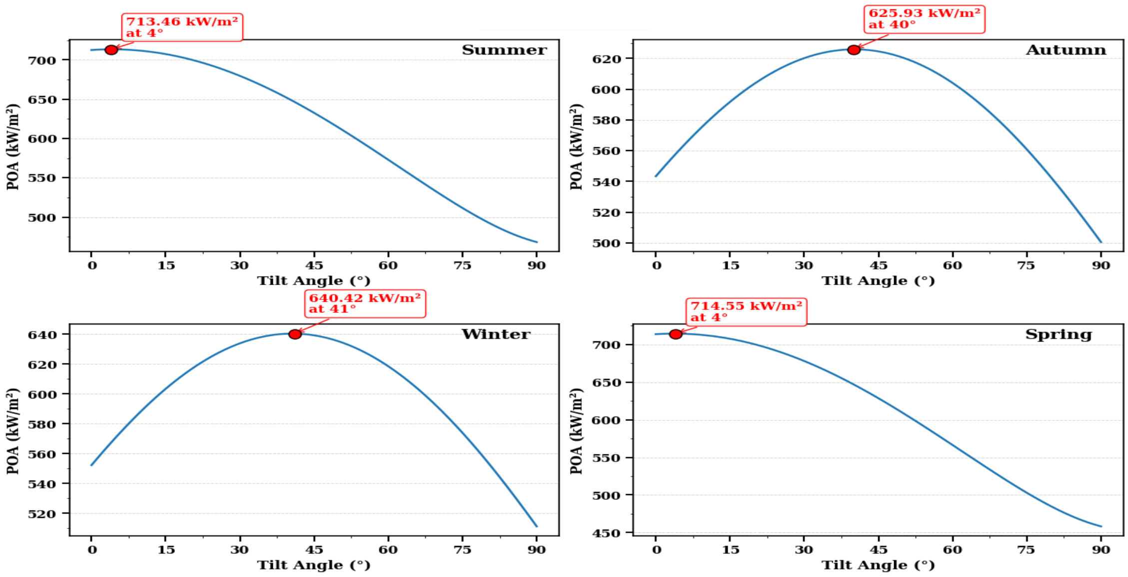

Figure 6. Optimum tilt angles for seasonal adjustable-tilt TSAT.

Moreover, the optimal tilt angle for monthly adjustable-tilt TSAT at each month is determined similarly by maximizing the POA value at the months from a 91×12 matrix, as shown in Figure 7.

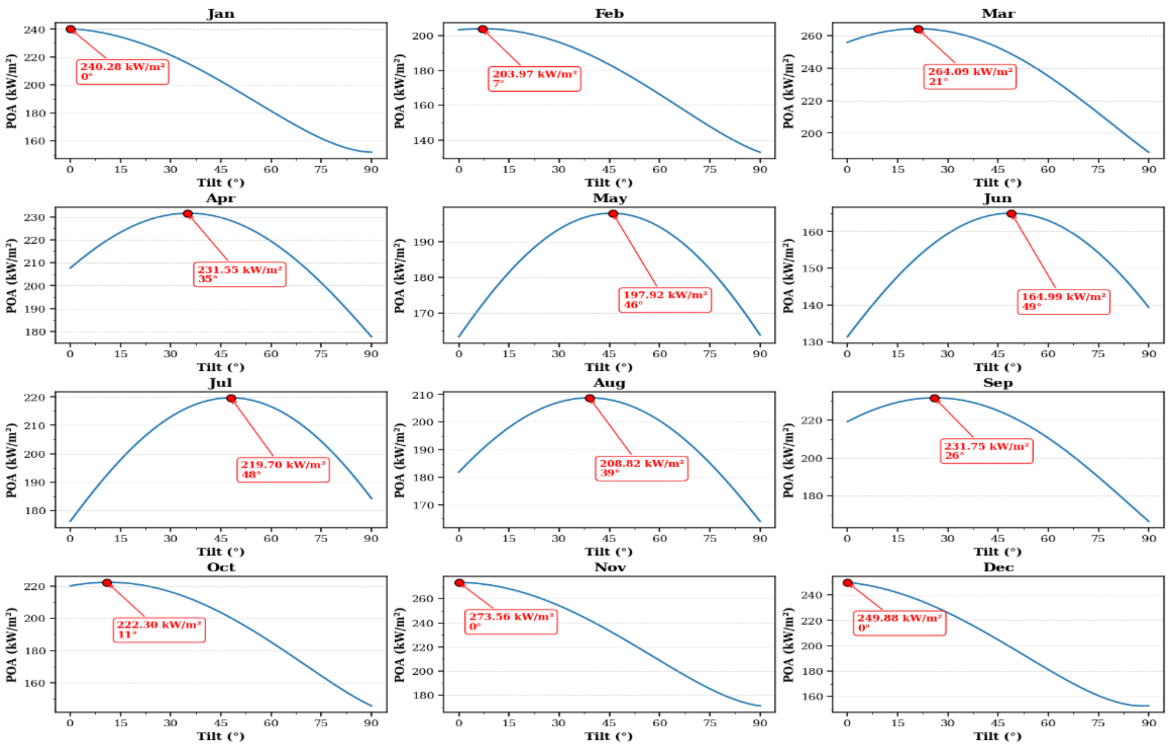

Figure 7. Optimum tilt angles for monthly adjustable-tilt TSAT.

3.1. Comparative analysis of adjustable-tilt TSAT and HSAT

By setting the TSAT at optimal tilt angles, their hourly POA values are calculated and aggregated to monthly, seasonal, and annual for comparison with the corresponding POA values of HSAT, as shown in Table 2.

Table 2. Comparison of adjustable-tilt TSATs with HSAT.

Period	HSAT	Annual adjustable-tilt TSAT		Seasonal adjustable-tilt TSAT		Monthly adjustable-tilt TSAT	
		POA_{opt}	Imp. %	POA_{opt}	Imp. %	POA_{opt}	Imp. %
Jan	240.27	228.23	-5.01	239.44	-0.34	240.28	0.00
Feb	203.28	200.14	-1.54	203.85	0.27	203.97	0.34
Mar	255.69	263.1	3.24	260.28	1.79	264.09	3.28
Apr	207.59	228.43	10.04	231.12	11.33	231.55	11.54
May	163.32	188.7	15.53	197.35	20.83	197.92	21.18
Jun	131.34	154.7	17.78	163.84	24.74	164.99	25.61
Jul	176.11	206.84	17.44	218.68	24.17	219.70	24.75
Aug	181.88	203.95	12.13	208.75	14.76	208.82	14.80
Sep	219.13	231.56	5.67	228.17	4.12	231.75	5.75
Oct	220.11	220	-0.52	221.37	0.57	222.30	0.99
Nov	273.55	261.71	-4.33	273.01	-0.2	273.56	0.00
Dec	249.88	234.17	-6.28	248.5	-0.55	249.88	0.00
Summer	712.62	695.33	-2.42	713.46	0.11	717.56	0.70
Autumn	543.38	609.7	12.21	625.93	15.19	628.98	15.75
Winter	552.33	622.66	12.73	640.42	15.94	643.99	16.60
Spring	713.8	694.7	-2.68	714.55	0.096	718.27	0.61
Years	2522.2	2622.45	3.97	2694.35	6.82	2708.81	7.40

Moreover, Figures 8 and 9 illustrate the comparison of aggregate monthly and seasonal POA values for 2020 across three types of TSATs: annual adjustable-tilt TSAT, seasonal adjustable-tilt TSAT, and monthly adjustable-tilt TSAT.

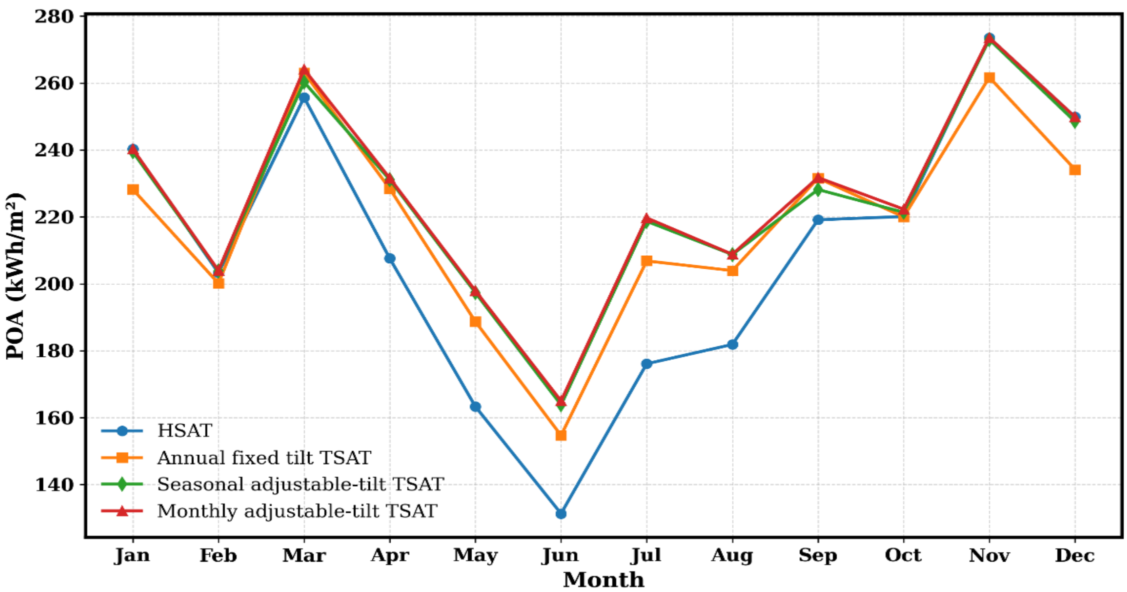

Figure 8. Comparison of the monthly aggregate POA for three types of TSATs against HSAT.

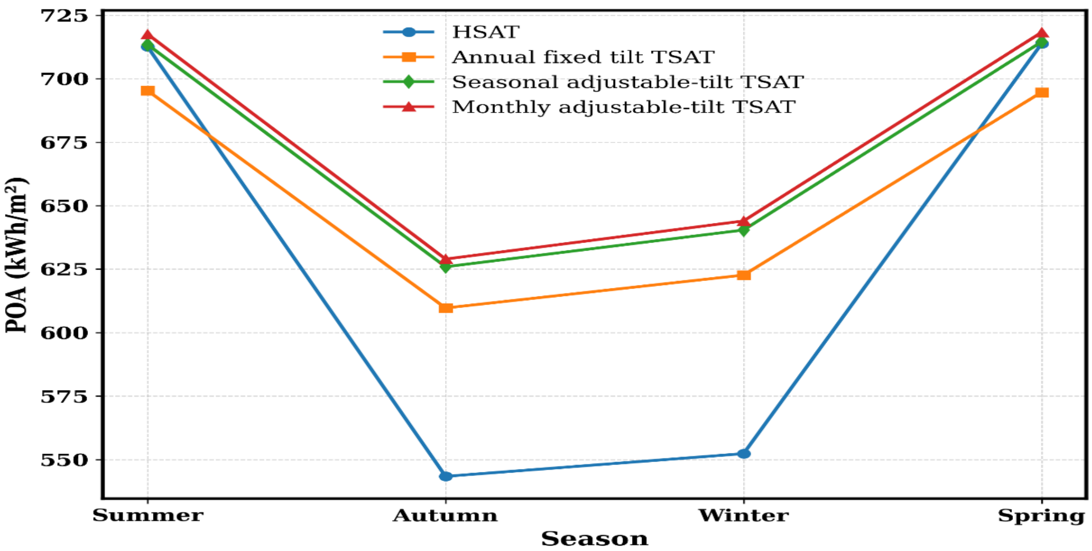

Figure 9. Comparison of the seasonal aggregate POA for three types of TSATs against HSAT.

4. Conclusion

This study investigates the use of adjustable-tilt TSATs to improve HSAT performance in capturing POA irradiance. Three TSAT configurations—annual adjustable-tilt, seasonal adjustable-tilt, and monthly adjustable-tilt—were designed, with their respective optimal tilt angles determined by maximizing the aggregate POA values over annual, seasonal, and monthly timescales.

Numerical simulations were conducted for a PV plant equipped with HSATs in Dracena, Brazil. Ground-truth data from this plant were used to identify the optimal combination of decomposition and transposition models, selected from an evaluation of 400 combinations. This optimal model combination was then applied to the plant's hourly GHI data to estimate the corresponding hourly POA values for adjustable-tilt TSATs, by varying the tilt angle from 0° to 90° in 1° increments. Subsequently, the optimal tilt angles for TSATs were determined for annual, seasonal, and monthly timescales. Finally, the annual adjustable-tilt, seasonal adjustable-tilt, and monthly adjustable-tilt TSAT configurations were set to their respective optimal tilt angles, and their performance was compared with that of the HSAT system.

Simulation results revealed that the TSAT configured at the annual optimal tilt does not consistently outperform the HSAT. In contrast, the monthly adjustable-tilt TSAT consistently demonstrated superior POA values, indicating its potential for improving solar energy capture efficiency. However, all three TSAT configurations outperform the HSAT during March, April, May, June, July, and September, with the maximum improvement observed for the monthly adjustable-tilt TSAT in June, achieving 25.61%.

5. Acknowledgments

This study was financed by TotalEnergies through the R&D incentive program of the Brazilian National Agency of Petroleum, Natural Gas and Biofuels (ANP) in partnership with CEPETRO and FEEC at UNICAMP.

6. References

ABSOLAR, 2025. Associação Brasileira de Energia Solar Fotovoltaica. Available at: https://www.absolar.org.br/.

Alomar, O.R., Ali, O.M., Ali, B.M., Qader, V.S., Ali, O.M., 2023. Energy, exergy, economical and environmental analysis of photovoltaic solar panel for fixed, single and dual axis tracking systems: An experimental and theoretical study. *Case Stud. Therm. Eng.*, 51, 103635.

Anderson, K., Hansen, C., Holmgren, W., Jensen, A., Mikofski, M., Driesse, A., 2023. pvlib python: 2023 project update. *J. Open Source Softw.*, 8(92), 5994.

Anderson, K., Mikofski, M., 2020. Slope-aware backtracking for single-axis trackers. Technical Report NREL/TP-5K00-76626, July.

Bahrami, A., Okoye, C.O., Atikol, U., 2017. Technical and economic assessment of fixed, single and dual-axis tracking PV panels in low latitude countries. *Renew. Energy*, 113, 563–579.

Bahrami, A., Okoye, C.O., Pourasl, H.H., Khojastehnezhad, V.M., 2022. Techno-economic comparison of fixed and tracking flat plate solar collectors in the northern hemisphere. *J. Clean. Prod.*, 378, 134523.

Berrian, D., Libal, J., Klenk, M., Nussbaumer, H., Kopecek, R., 2019. Performance of bifacial PV arrays with fixed tilt and horizontal single-axis tracking: Comparison of simulated and measured data. *IEEE J. Photovolt.*, 9(6), 1583–1589.

Campion, N., Montanari, G., Guzzini, A., Visser, L., Alcayde, A., 2025. Green hydrogen techno-economic assessments from simulated and measured solar photovoltaic power profiles. *Renew. Sustain. Energy Rev.*, 209.

De Souza Silva, J.L., Da Silva, J.A.F.G., Mahmoudi, E., De Paula, J.F.S., Dos Santos Barros, T.A., Villalva, M.G., 2023. Evaluating the significance of solarimetric data for photovoltaic system simulation in a real-world case. In: *Proc. 2023 IEEE 8th Southern Power Electronics Conf. (SPEC) and 17th Brazilian Power Electronics Conf. (COBEP)*, Florianópolis, Brazil, pp. 1–6.

De Souza Silva, J.L., Mahmoudi, E., Carvalho, R.R., Dos Santos Barros, T.A., 2024. Classification of anomalies in photovoltaic systems using supervised machine learning techniques and real data. *Energy Rep.*, 11, 4642–4656.

De Souza Silva, J.L., Mahmoudi, E., Paula, J.F., Barros, T.A., 2025. Case study on photovoltaic system: Impact of solarimetric stations on simulations and anomaly detection. *Eletrônica de Potência*, 30, e202506.

Gönül, Ö., Yazar, F., Duman, A.C., Güler, Ö., 2022. A comparative techno-economic assessment of manually adjustable tilt mechanisms and automatic solar trackers for behind-the-meter PV applications. *Renew. Sustain. Energy Rev.*, 168, 112770.

Gueymard, C.A., Ruiz-Arias, J. A., Extensive worldwide validation and climate sensitivity analysis of direct irradiance predictions from 1-min global irradiance, Solar Energy,Volume 128, Pages 1-30, 2016.

Li, Z., Liu, X., Tang, R., 2010. Optical performance of inclined south–north single-axis tracked solar panels. *Energy*, 35(6), 2511–2516.

Mahmoudi, E., Dos Santos Barros, T.A., Alvarez, H., Garcia, R., Marques, F.C., Villalva, M.G., 2023. The effect of tilt and azimuth angle variations on monthly and annual incident solar radiations for locations in Brazil. In: *Proc. 2023 IEEE 50th Photovoltaic Specialists Conf. (PVSC)*, San Juan, PR, USA, pp. 1–7.

Mahmoudi, E., Nunes, I., Neves, M.R.M., Garcia, R., Marques, F.C., Villalva, M.G., Dos Santos Barros, T.A., 2023. Assessing the influence of tilt and azimuth angle variations on plane of array irradiance in Brazilian cities. *Proc. EU PVSEC 2023*, DOI:10.4229/EUPVSEC2023/4CV.1.46.

Ray, S., Tripathi, A.K., 2016. Design and development of tilted single-axis and azimuth–altitude dual-axis solar tracking systems. In: *Proc. IEEE 1st Int. Conf. Power Electron., Intell. Control Energy Syst. (ICPEICES)*, Delhi, India, pp. 1–6. DOI:10.1109/ICPEICES.2016.7853190.

Sanyal, A., Mohanta, J.C., Faiyaz, A.M.D., 2024. Development of a dual-axis solar tracker for efficient sun energy harvesting. *Proc. Inst. Mech. Eng. Part E: J. Process Mech. Eng.*, 1, Apr.